

## Supplementary data and figures

### Thyroid hormone inhibits murine lung fibrosis through improved epithelial mitochondrial function

Guoying Yu<sup>1\*</sup>, Argyris Tzouveleki<sup>1,2\*</sup>, Rong Wang<sup>1</sup>, Jose D. Herazo-Maya<sup>1</sup>, Gabriel H. Ibarra<sup>1</sup>, Anup Srivastava<sup>1</sup>, Joao Pedro Werneck de Castro<sup>3,4</sup>, Giuseppe DeLuliis<sup>1</sup>, Farida Ahangari<sup>1</sup>, Tony Woolard<sup>1</sup>, Nachele Aurelien<sup>1</sup>, Rafael Arrojo e Drigo<sup>5</sup>, Ye Gan<sup>1</sup>, Morven Graham<sup>6</sup>, Xinran Liu<sup>6</sup>, Robert J. Homer<sup>7,8</sup>, Thomas S. Scanlan<sup>9</sup>, Praveen Mannam<sup>1</sup>, Patty J. Lee<sup>1</sup>, Erica L. Herzog<sup>1</sup>, Antonio C. Bianco<sup>3</sup>, Naftali Kaminski<sup>1</sup>

\*These authors contributed equally to work

<sup>1</sup>Section of Pulmonary, Critical Care and Sleep Medicine, Department of Internal Medicine, Yale School of Medicine, New Haven, CT,

<sup>2</sup>Division of Immunology, Biomedical Sciences Research Center “Alexander Fleming”, Athens, Greece

<sup>3</sup>Division of Endocrinology/Metabolism, Rush University Medical Center, Chicago IL

<sup>4</sup>Biophysics Institute, Federal University of Rio de Janeiro, RJ, Brazil

<sup>5</sup>The Salk Institute for Biological Studies, Molecular and Cell biology laboratory, La Jolla, CA

<sup>6</sup>CCMI Electron Microscopy Core Facility, Yale University School of Medicine, New Haven, CT

<sup>7</sup>Department of Pathology, Yale University School of Medicine, New Haven, C

<sup>8</sup>Pathology and Laboratory Medicine Service, VA CT HealthCare System, West Haven, CT

<sup>9</sup>Department of Physiology and Pharmacology, Oregon Health and Science University, Portland, Oregon, USA

Correspondence to:

Naftali Kaminski MD,

Pulmonary, Critical Care and Sleep Medicine, Yale School of Medicine, New Haven, CT

Email: [naftali.kaminski@yale.edu](mailto:naftali.kaminski@yale.edu)

Keywords: Pulmonary Fibrosis, Mitochondria, Thyroid Hormone, Sobiterome, Alveolar epithelial Cells

**Table S1. Demographics and clinical characteristics of the LGRC cohort**

Characteristic	IPF ( <i>n</i> = 123)	Control ( <i>n</i> = 96)
Age (yr) (Mean ± SD)	64.8 ± 8.3	63.8 ± 11.2
Gender, <i>n</i> (%)		
Males	82 (66.7)	46 (47.9)
Females	41 (33.3)	50 (52.1)
Race, <i>n</i>		
White	113	88
African-American	5	3
Hispanic	1	2
Asian or pacific islander	2	1
Native American	0	1
Not disclosed	2	1
Pulmonary function tests (mean ± SD)		
FVC%	65 ± 16	95 ± 13
DLCO%	48 ± 18	83 ± 17
FEV1%	71 ± 16	95 ± 13

\*FVC%: Forced vital capacity percent predicted, DLCO%: Carbon monoxide diffusing capacity percent predicted. FEV1% Forced expiratory volume in 1 second percent predicted.

## Supplementary Figure Legends

**Supplementary Figure 1** Systemic T4 administration attenuates established bleomycin-induced lung fibrosis. **(a)** Collagen deposition in mice treated with T4 was assessed by hydroxyproline content. Data presented are from one of two independent experiments with similar results and are expressed as mean hydroxyproline content per lung set  $\pm$  SEM,  $*P = 0.002$ . **(b, c)** Quantitative RT-PCR analysis of collagen type 1, alpha 1 (*Col1a1*), type 3, alpha 1 (*Col3a1*) mRNA levels (means  $\pm$  SEM) in mice treated with T4 or T3,  $*P = 0.001$ ,  $*P < 0.001$ , respectively, **(d)** Serum T3 levels in mice treated with saline, bleomycin and bleomycin+T4. Data are presented as box-and-whisker plots with horizontal bars representing mean T3 serum levels (ng/ml)  $\pm$  SEM,  $\#P = 0.04$ . **(e)** Masson's Trichrome staining of representative lung sections ( $n = 5$ ) from each group of treated mice. Statistical tests used one-way ANOVA with Student-Newman-Keuls post-hoc test for pairwise comparisons **(b,c)** ( $F=9.2, 18.5, 2.9$ , and  $df=20, 18$  and  $33$ , respectively) and Student's t-test for independent samples **(d)** ( $t$  statistic=2.2 and 2.1 respectively).

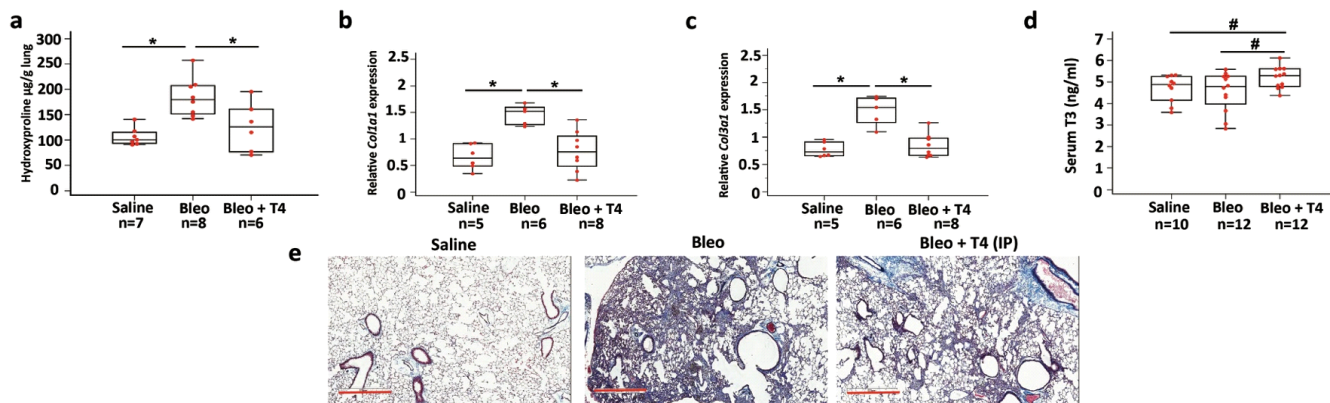
**Supplementary Figure 2** TH treatment restores bleomycin-induced mitochondrial bioenergetics abnormalities in lung epithelial cells *in-vivo* and *in-vitro*. **(a)** Beneficial effects of *in-vivo* T3 on mitochondrial function parameters in AECIIs isolated from 9-12 weeks-old C57/BL6 female mice treated daily with aerosolized T3 following intratracheal challenge with bleomycin or equivalent volume of normal saline. Mitochondrial function was assessed by measuring oxygen consumption rate. Data are presented as box-and-whisker plots with horizontal bars representing mean  $\pm$  SEM,  $*P < 0.001$ . **(b-d)** *In-vivo* beneficial effects of T3 treatment in mitochondrial bioenergetic profile were further validated *in-vitro* in three different types of lung epithelial cells, including human small airway epithelial cells-SAECs, primary mouse AECIIs and mouse lung epithelial cells-MLE-12. Cells were seeded into 96-well plates (40,000/well), exposed to bleomycin (15 mU/ml) or PBS for 4 hours and then treated with T3 (15 ng/ml)

or empty vehicle for 8 hours. Administration of T3 significantly improved bleomycin-induced mitochondrial function abnormalities as indicated by significant increases in mitochondrial and basal respiration, as well as ATP production, coupling efficiency and proton leak. Data are presented as box-and-whisker plots with horizontal bars representing mean $\pm$  SEM, \* $P < 0.001$ . Statistical test used one-way ANOVA with Student-Newman-Keuls post-hoc test for pairwise comparisons, \* $P < 0.001$ . Statistical tests used one-way ANOVA with Student-Newman-Keuls post-hoc test for pairwise comparisons (a) (OCR) (F=91.4, df=42), basal respiration (F=13.6, df=44), ATP production (F=27.8, df=44), coupling efficiency (F=25.8, df=44), proton leak (F=25.7, df=44). (b-d) mitochondrial (F=30.1, 39.7, 74.6 and df=74, 88, 87, respectively) and basal respiration (F=19.7, 18.9, 64.5 and df=74, 88, 87 respectively), ATP production (F=15.3, 21.6, 66.7 and df=74, 88, 87) coupling efficiency (F=25.4, 5.2, 43.2 and df=74, 88, 87) and proton leak (F=34.8, 9.6, 74.4 and df=74, 88, 87, respectively).

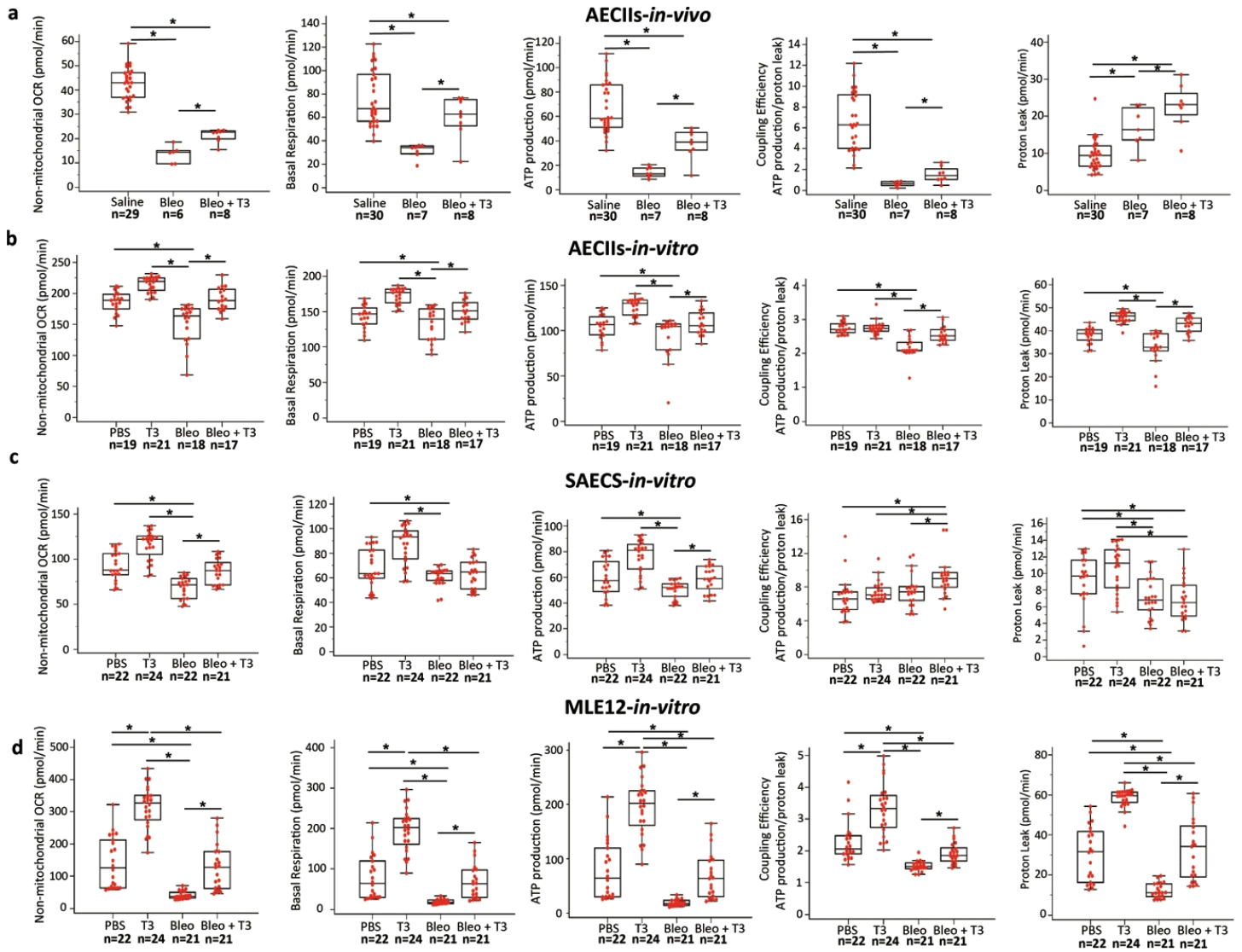
**Supplementary Figure 3** PPARGC1A is decreased in patients with idiopathic pulmonary fibrosis (a) Quantitative RT-PCR analysis of the *PPARGC1A* mRNA levels (means $\pm$  SEM) in whole IPF lungs ( $n = 17$ ) and controls ( $n = 17$ ), \* $P = 0.004$ . (b) Immunoblot of IPF whole lung lysates ( $n = 4$ ) showing PPARGC1A protein levels compared to control lungs ( $n = 4$ ) (upper panel). Immunoblot gels were cropped. (c, d) Immunohistochemistry analysis in representative lung tissue samples showing increased PPARGC1A expression in IPF lung compared to control. Scale bars 100  $\mu\text{m}$ . Statistical test used was Mann-Whitney U-test for independent samples ( $z=2.8$ ).

**Supplementary Figure 4** Uncropped images of the immunoblot gels. **Part 1** (a) Uncropped images for Figure 1d. (b) Uncropped images for Figure 3n (SAECs). (c) Uncropped images for Figure 3n (ATIIs). (d) Uncropped images for Figure 3n (MLE12). **Part 2** (e) Uncropped images for Figure 4a (SAECs). (f)

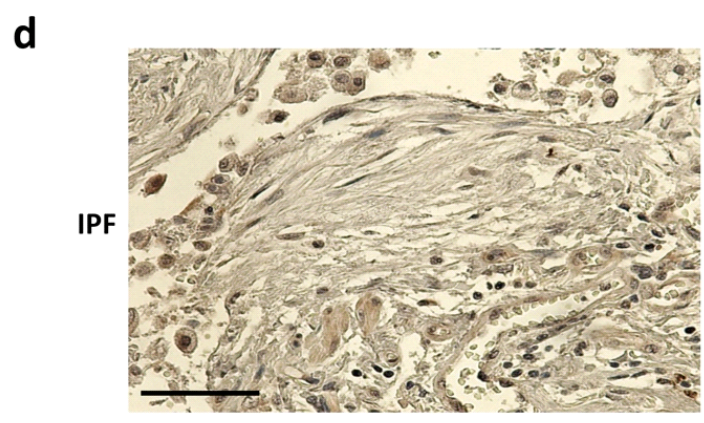
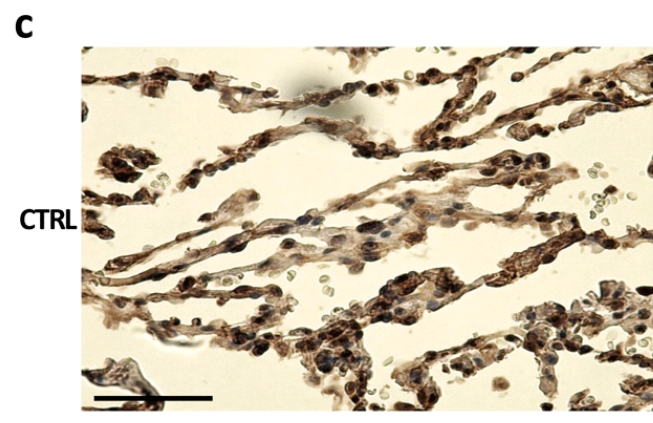
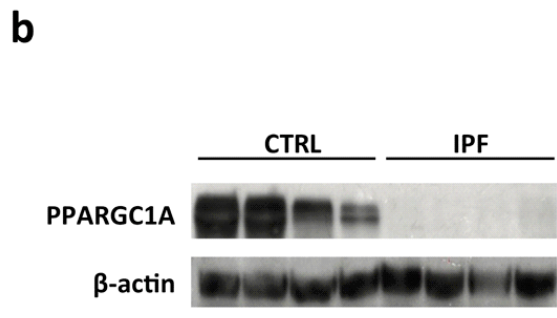
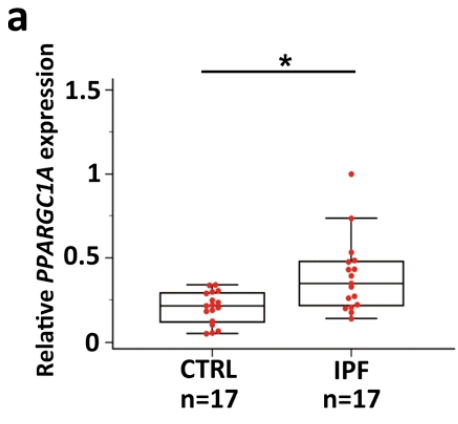
Uncropped images for Figure 4a (ATIIIs). (g) Uncropped images for Figure 4a (MLE12). (h) Uncropped images for Figure 5g. (i) Uncropped images for Supplementary figure 3c.



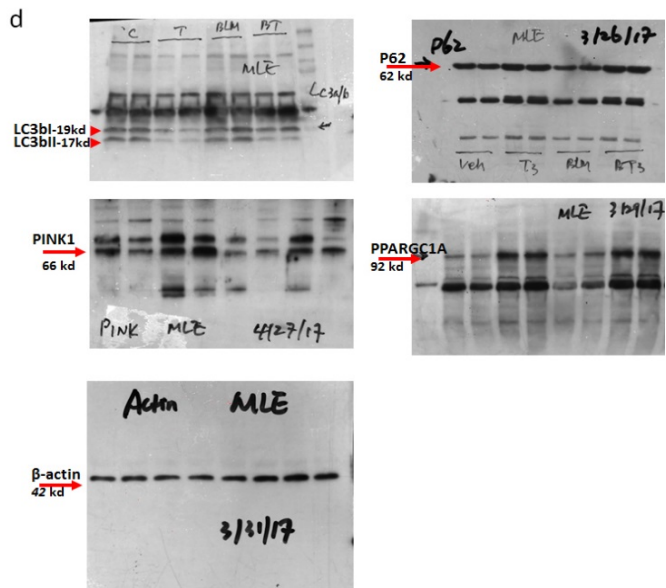
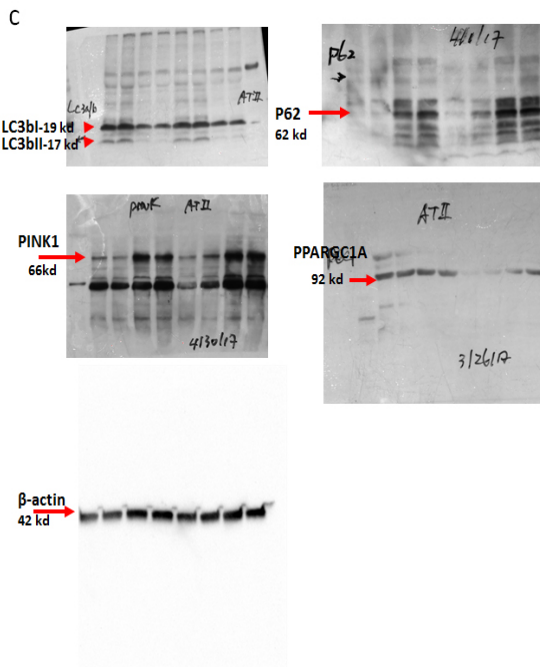
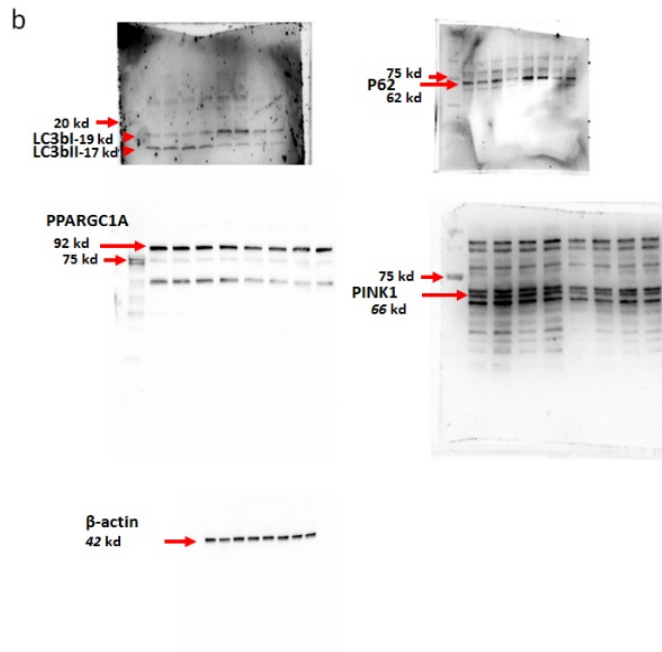
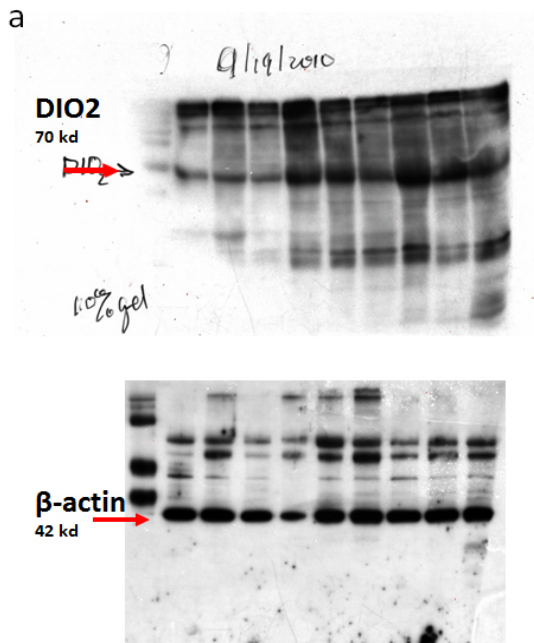
Supplementary Figure 1



Supplementary Figure 2



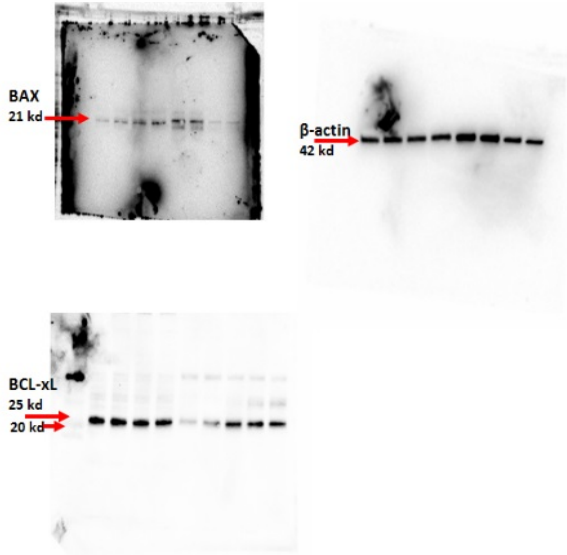
Supplementary Figure 3



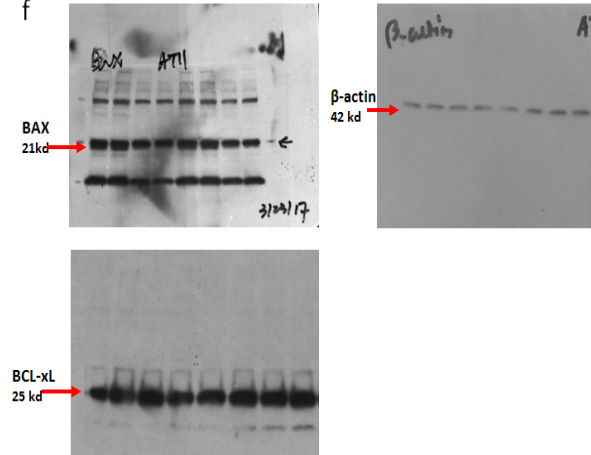
Supplementary Figure 4 (part 1)



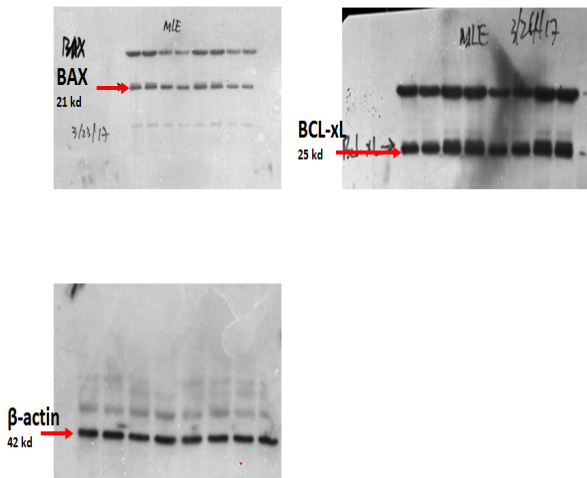
e



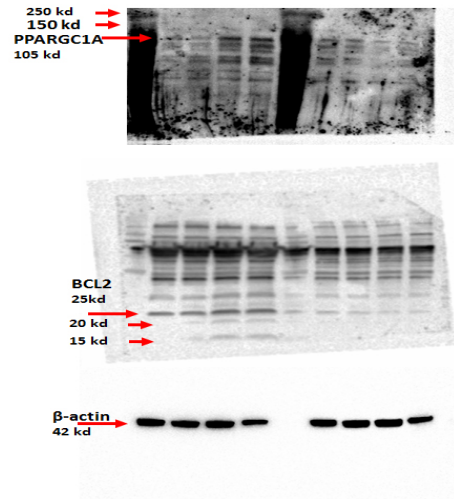
f



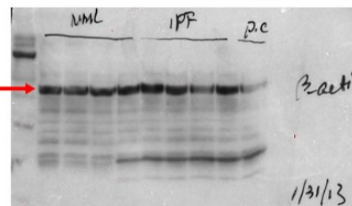
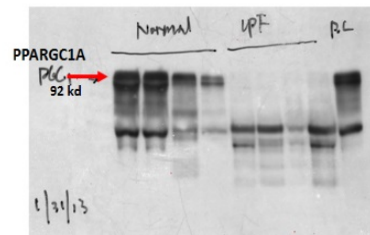
g



h



i



Supplementary Figure 4 (part 2)